Simulation And Implementation Of High Step-Up Ratio Flyback Converter With Voltage Multiplier And Active Clamp

Associate Prof. Nalini S
Department of Electrical and Electronics
Dr. Ambedkar Institute of Technology
Bangalore, India

Hamsa Rekha S D
Department of Electrical and Electronics
Dr. Ambedkar Institute of Technology Bangalore, India

Abstract

In this paper, an isolated high step up ratio dc-dc converter aimed to be used in interface systems between low voltage renewable energy sources like photovoltaic panels, fuel cells and utility grid is proposed. The converter is based on the active clamp flyback topology at the primary side of the transformer with a voltage multiplier at the secondary side of the transformer. By natural clamping the rectifier diode voltages the use of dissipative snubber circuit is avoided. The auxiliary switch and clamp capacitor are used in primary side to recycle the energy stored in the transformer in order to minimize the spike voltage by which the voltage stress on the main switch can be reduced. The voltage multiplier configuration, allows to naturally clamp the rectifier diode voltages.

1. Introduction

High step-up ratio converters able to efficiently interface low-voltage high-current energy sources like batteries and renewable energy sources like photovoltaic panels, fuel cells with the utility grid are nowadays the focus of an intensive research effort by the power electronics community. These converters find applications in almost all power electronic systems. The simple boost converter has been proved to be insufficient in providing high step-up ratios in an efficient way, due to the high current and voltage stress on the switch and the severe diode reverse recovery losses, when operating in continuous conduction mode. Thus, different topologies have been investigated in literature to overcome these drawbacks. In [1], for example, the use of voltage multiplier cells cascaded with a single-phase and/or a multi- phase boost converter has been proposed. The solution is interesting, because of the continuous input current and the reduced switch voltage stress, the diode reverse recovery affects the overall efficiency, but it requires additional resonant inductors to cope with the diode reverse recovery problem.

Further, the use of coupled inductors associated with the boost power stage has been widely investigated. These topologies, called as integrated boost-flyback (IBF) converters, introduce a degree of freedom associated with the coupled inductor turns ratio, that allows to boost the output voltage while keeping the switch voltage stress at a reasonable level [2]. These converters require suitable voltage clamping on the rectifier diodes to limit their voltage stress. It has been demonstrated in [3] and [4] that the resonance caused by the transformer leakage inductances and the diode parasitic capacitances strongly modifies the converter behaviour, introducing an additional boost action that helps to increase the overall converter's voltage gain.

The flyback converter with active clamp seems a promising topology able to combine isolation with soft commutations [5].

In this paper, an isolated version of the topology presented in [5] is proposed, based on a flyback converter that employs an active clamp, at the transformer primary side, and a voltage multiplier at the transformer secondary side. The resonant phases between the transformer leakage inductances and the diode parasitic capacitances have a beneficial effect of reducing the circulating current through the active clamp, thus lowering the conduction losses during the turn off interval of the main switch. Moreover, clean rectifier diode voltage waveforms are obtained at the transformer secondary side due to the clamping action of output diodes.

International Journal of Engineering Research & Technology (IJERT)
ISSN: 2278-0181
Vol. 2 Issue 5, May - 2013

2. Block diagram implemented

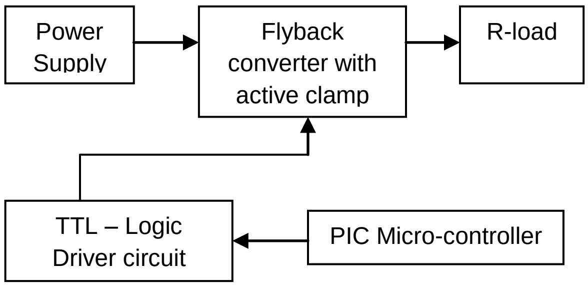

Figure 1. Block diagram of flyback converter with active clamp and voltage multiplier

The above Figure 1 shows the block diagram of the flyback converter with active clamp and voltage multiplier to be implemented. A PIC 16F877 micro-controller IC is given to the driver circuit in which TTL-logic is used and the driver circuit drives the flyback converter with active clamp and the voltage multiplier in which the proposed circuit is tested using the MATLab Simulink software with R-load. The power supply is given to the proposed circuit with the input voltage of 30V and obtaining the output of 400V.

3. Flyback converter with active clamp and voltage multiplier

Figure 2 shows the scheme of proposed Flyback converter with active clamp and voltage multiplier highlighting major parasitic components. In the attempt to regain isolation capability while keeping the ability of processing the leakage inductance energy in a loss-less manner, a flyback cell with active clamp and voltage multiplier, is proposed as shown in Figure 2 where the major parasitic components, i.e. primary and secondary transformer leakage inductances Ld and Ls, rectifier diode D1 and D2 capacitances grouped into one equivalent capacitance Cr = Cd1+Cd2, are highlighted. Simulated results reports the converter main waveforms in a switching period.

Assuming that the flyback section operates in CCM. Each switching period can be divided into six subintervals. In the analysis of the circuit, the small resonant intervals corresponding to the charge and discharge of the switch output capacitances occurring during the dead times in the switch commands are neglected, being their duration very small compared to the switching period.

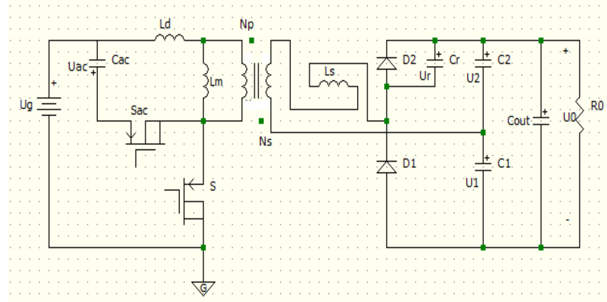

Figure 2. Circuit configuration of proposed active clamp flyback converter with voltage multiplier

Each switching period can be divided into six subintervals i.e. T_{01}, T_{12}, T_{23}, T_{34}, T_{45} and T_{56}.

3.1. Interval $T_{01} = t_1\text{-}t_0$

Prior to the interval T_{01}, diode D_2 is conducting and the energy stored in the magnetizing inductance is being transferred to capacitor C_2 and the load. At t_0, the main switch S is turned on causing current id to increase and D_2 current to decrease accordingly. Being D_2 still conducting, the magnetizing current continues to decrease.

3.2. Interval $T_{12} = t_2\text{-}t_1$

At t_1, when the input current equals the magnetizing one, diode D_2 turns off allowing a resonance to occur. Here, as already stated above, the resonant capacitance Cr accounts for both D_1 and D_2 parasitic capacitances. The resonance phase ends as soon as voltage ur(t) equals the output voltage $U_0 = U_1+U_2$, causing the turn on of diode D_1.

3.3. Interval $T_{23} = t_3\text{-}t_2$

The corresponding currents vary linearly. When D_1 is turned on, the actual slope of current id depends on the converter operating point. By neglecting the resonance stage, diode D_1 would be conducting during the switch on time, the presence of the parasitic components causes a non-zero D_1 current. In the latter case, D_1 current will simply have a negative current slope, meaning that it can go to zero before the end of the switch on-time, thus causing the turn off of diode D_1. In the following analysis, it is assumed that D_1 conducts for the whole switch on time interval. Note that this interval corresponds to an energy transfer to inner output voltage U_1 in a forward manner, with the current limited by the total transformer leakage inductance.

3.4. Interval $T_{34} = t_4 - t_3$

At instant t_3, the main switch S is turned off, causing the conduction of the auxiliary switch body diode D_{AC}. During this interval, diode D_1 is still conducting. Here, it is assumed that the clamp capacitor C_{AC} is sufficiently big to keep its voltage almost constant during the switching period. The leakage inductance current rapidly decreases, while the magnetizing one continues to increase. At t_4, the input current equals the magnetizing one, and diode D_1 current goes to zero, causing its turning off of D_1.

3.5. Interval $T_{45} = t_5 - t_4$

At instant t_4, the input current equals the magnetizing one and the diode D_1 becomes zero i.e when D_1 turns off a second resonance occurs that brings the resonant capacitor voltage to zero, thus turning on diode D_2. At instant t_5, the resonant voltage becomes zero and diode D_2 turns on.

3.6. Interval $T_{56} = t_6 - t_5$

At instant t_5, Diode D_2 turns on and the energy stored in the magnetizing inductance is delivered to the flyback's output U_2, while the leakage inductance energy continues to be exchanged with the clamp capacitor. Both leakage inductance and magnetizing currents decrease linearly and the inductor currents follow a resonant behaviour. In any case, current id reverts its direction flowing through the auxiliary switch S_{AC}.

4. Driver circuit

Driver circuit helps to drive the voltage and give it to the flyback converter with the active clamp and voltage multiplier. Figure 3 indicates the schematic representation of the driver circuit. The driver circuit consists of opto-coupler, step down transformer, PNP and NPN transistors, diode and filtering capacitor. The output is given to the switch i.e to the MOSFET of the proposed converter.

Initially the input is given by the controller to the opto-coupler and the output from the opto-coupler is given to the PNP transistor due to the transient response of the transistor 12V output is obtained if this fails to give 12V NPN transistor helps us to obtain 12V output in which the collector side of the transistor is driven from the output of the step-down transformer by using forward biased diode and the capacitor. The output of the driver circuit is given as gating pulse to the MOSFET.

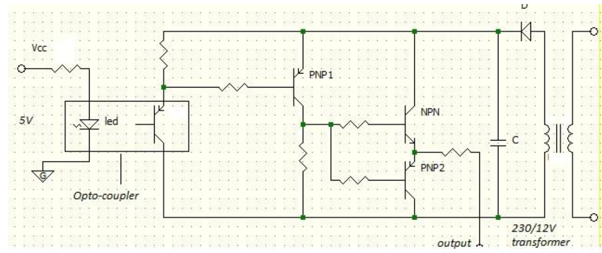

Figure 3. Schematic representation of driver circuit

4.1. Opto – coupler

Opto-isolators, or opto-couplers, are made up of a light emitting device, and a light sensitive device, all wrapped up in one package, but with no electrical connection between the two, just a beam of light. The light emitter is nearly always an LED. The light sensitive device may be a photodiode, phototransistor, or more esoteric devices such as thyristors, triacs etc.

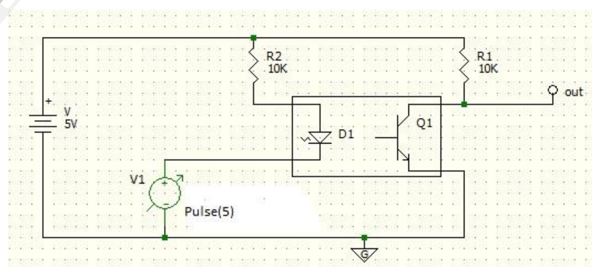

Figure 4. schematic representation of opto-coupler

When the LED is driven with a current of 10mA, it shines onto the phototransistor, which then starts to conduct (turn on). This takes the output voltage low. However much electrical noise is on one side, it can never be transmitted over to the other side. We may use an opto-isolator to send PWM signals from the low-power electronics side to the MOSFET drivers on the high-power side, and we may use them to transmit information from the high- power side back to the low-power side.

4.1.1. Collector-emitter voltage : This is the maximum voltage that can be present from the collector to the emitter of the receiving phototransistor (when it is turned off - no light) before it may break-down.

ISSN: 2278-0181
Vol. 2 Issue 5, May - 2013

4.1.2. Creepage distance : This is physically how far a spark would have to travel around the outside of the package to get from one side to the other. If the package has contaminants on it, solder flux, or dampness, then a lower-resistance path can be created for noise signals to travel along.

4.1.3. Forward current : This is the current passing through the sending LED. Typically, an opto-isolator will require about 5mA to turn the output transistor on.

4.1.4. Forward voltage : This is the voltage that is dropped across the LED when it is turned on. Most normal diodes drop about 0.7v, but with LEDs it is typically 1 - 2 volts.

4.1.5. Collector dark current : This is the current that can flow through the output phototransistor when it is turned off.

4.1.6. Collector-emitter saturation voltage : When the output transistor is fully turned on (saturated), this is the voltage there will be between the collector and emitter.

4.1.7. Isolation resistance : This is the resistance from a pin in the input side to a pin on the output side. It should be very high.

4.1.8. Response time : Thee rise and fall times are the times that the output voltage takes to get from zero to maximum. The rise time is very much dependant on the load resistor, since it is this that is pulling the output up. Therefore this value is always quoted with a fixed load resistance. Note however that the value, 100 Ohms, is much less than you are likely to use in practice.

4.1.9. Cut-off frequency : This is effectively the highest frequency of square wave that can be sent through the opto-isolator. It is actually the frequency at which the output voltage is only swinging half the amplitude than at DC levels (-3dB = half). It is therefore linked with the rise and fall times.

4.1.10. Current Transfer Ratio (CTR) : This is the ratio of how much collector current in the output transistor that you get given a certain amount of forward current in the input side LED. It is affected by how close the LED and phototransistor are inside the device, how efficient they both are, and many other factors. In fact it is not a constant but varies wildly with LED forward current.

5. Micro-controller

PIC Micro-controller is used to give the input to the opto-coupler of the driver circuit of 5V through buffer to improve the current rating of the circuit. Figure 4 shows connection from micro-controller to the driver circuit.

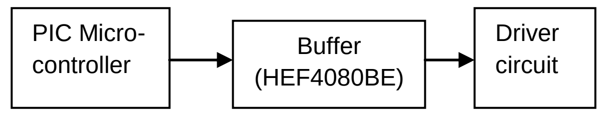

Figure 4. Connection between micro-controller and driver circuit

The buffer IC which is used in between the micro-controller and driver circuit increases the current rating of the controller output.

Figure 5 shows the pin diagram of the PIC micro-controller 16F877. In this we will use one of the port output as the input to the opto-coupler which gives the output as 5V.

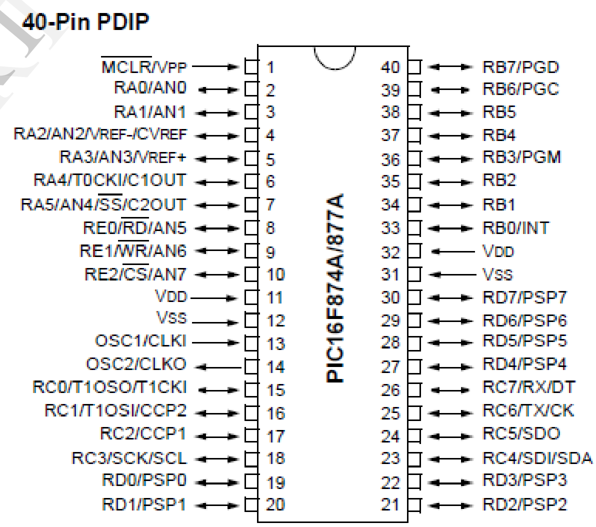

Figure 5. Pin diagram of PIC 16F877

From Figure 5 we can see that the power is given to VCC and input is taken from one of the port. The features of PIC 16F877 are shown in Table 1.

Table 1. Features of PIC 16F877

Key features	16F877
Operating frequency	DC-20MHz
Resets (and Delays)	POR,BOR (PWRT,OST)
Flash program memory (14-bit words)	8K
Data memory(bytes)	368
EEPROM data memory(bytes)	256
Interrupts	15
I/O ports	Ports A,B,C,D,E
Timers	3
Capture/compare/PWM modules	2
Serial communications	MSSP,USART
Parallel communications	PSP
10-bit A/D module	8 input channels
Analog comparators	2
Instruction set	35 instructions
Packages	40 pin PDIP 40 pin PLCC 40 pin TQFP 40 pin QFN

6. Simulation result for proposed circuit

The simulation results using MATLAB Simulink for the proposed circuit is shown below, Figure 6 shows the current at the primary side of the transformer i.e. input current and magnetizing current, Figure 7 shows the current across the diode D1, Figure 8 shows the current across diode D2, Figure 9 shows the Voltage across diode D1 and D2 and Figure 10 shows the output of the proposed circuit.

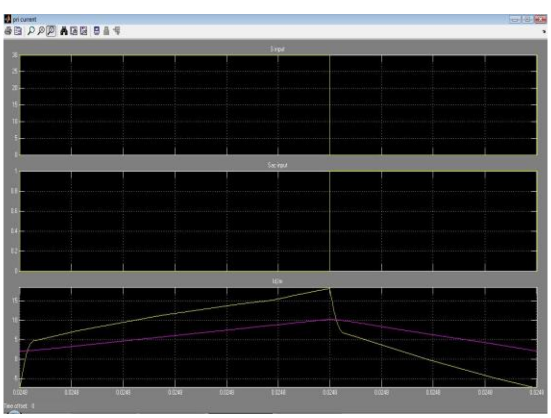

Figure 6. Waveforms of input current and magnetizing current

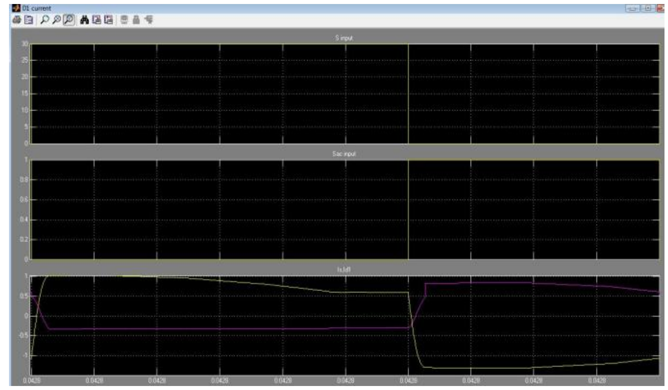

Figure 7. Waveform of current across Diode D1

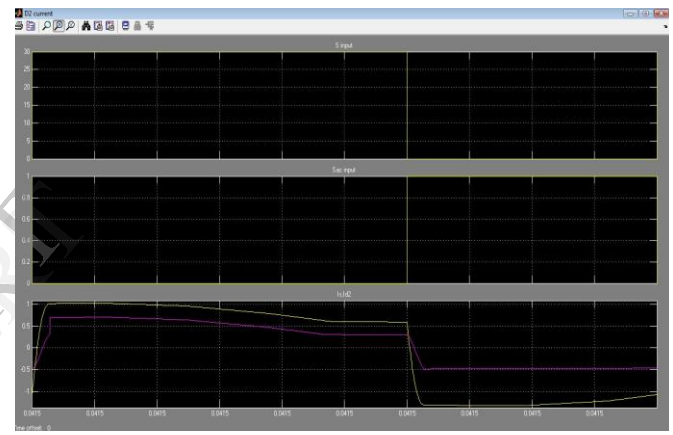

Figure 8. Waveform of current across Diode D2

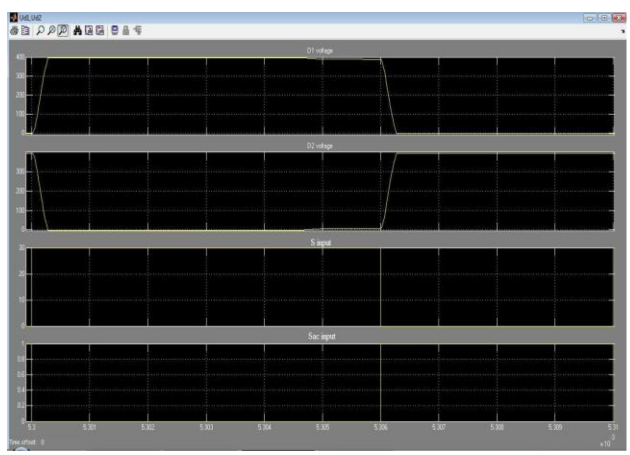

Figure 9. Waveform of voltage across Diode D1 and D2

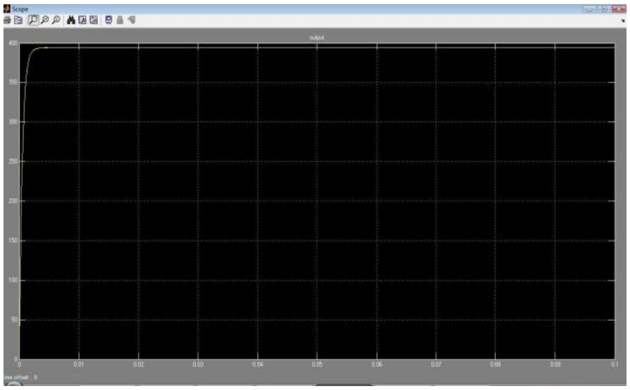

Figure 10. Waveform of Output of Proposed circuit

7. Conclusion

An isolated high step-up ratio dc-dc converter based on the active clamp flyback topology with a voltage multiplier at the secondary side has been proposed. The primary side active clamp guarantees a proper recirculation of the leakage inductance energy while providing zero voltage turn on of the main switch. The voltage multiplier configuration, allows to naturally clamp the rectifier diode voltages, thus avoiding the use of dissipative snubber circuits. Moreover, it is shown that the resonance involving the transformer leakage inductances and the diode parasitic capacitances allows the reduction of the circulating current during the active clamp operation, thus increasing the overall converter efficiency.

8. References

[1] M. Prudente, L. L. Pfitscher, G. Emmendoerfer, E. F. Romaneli, and R. Gules, “Voltage Multiplier Cells Applied to Non-Isolated DC–DC Converters,” IEEE Transactions on Power Electronics, Vol. 23, No. 2, March 2008, pp. 871–887.D.

[2] T. J. Liang, K. C. Tseng, “Analysis of integrated boost-flyback step-up converter,” IEE Proc. Electr. Power Appl., Vol. 152, No. 2, March 2005, pp. 217–225.

[3] G. Spiazzi, P. Mattavelli, A. Costabeber, “Effect of Parasitic Components in the Integrated Boost-Flyback High Step-Up Converter,” IEEE Annual Conference on Industrial Electronics (IECON), Porto (Portugal), November 2009, pp. 420-425.M.

[4] G. Spiazzi, P. Mattavelli, J. R. Gazoli, R. Magalhaes, G. Frattini, “Improved Integrated Boost-Flyback High Step-Up Converter,” IEEE International Conference on Industrial Technology (ICIT), Valparaiso (Chile), March 2010, pp. 1169-1174.

[5] B. R. Lin, H. K. Chiang, K. C. Chen, D. Wang, “Analysis, design and implementation of an active clamp flyback converter,” IEEE PEDS, 2005, pp. 424–429.

International Journal of Engineering Research & Technology (IJERT)

ISSN: 2278 - 0181

(ESRSA Publication)

COPYRIGHT AGREEMENT

Please complete and sign the form and send it with the final version of your manuscript. It is required to obtain written confirmation from authors in order to acquire copyrights for papers published in the journal so as to index them to various repositories.

Title of paper:

Simulation and Implementation of High Step-Up Ratio Flyback Converter with Voltage Multiplier and Active Clamp

Author(s): Hamsa Rekha S D, Nalini S

The undersigned hereby transfer any and all rights in and to the paper including without limitation all copyrights to the IJERT (ESRSA Publication). The undersigned hereby represents and warrants that the paper is original and that he/she is the author of the paper, except for material that is clearly identified as to its original source, with permission notices from the copyright owners where required. The undersigned represents that he/she has the power and authority to make and execute this assignment.

This agreement is to be signed by at least one of the authors who have obtained the assent of the co-author(s) where applicable.

Hamsarekha sd and 06/05/2013

Author's Signature & Date

Hamsa Rekha S D, Nalini S